



# **Universidad de Monterrey**

**Facultad de Ingeniería y Tecnología  
Ingeniería en Sistemas Computacionales**

## **Automatic classification of plutonic rocks with machine learning applied to extracted colors on iOS devices**

**Sarah Hernández Serrano  
1170469**

**Asesor: Dr. Germán Harvey Alférez Salinas  
Asesores secundarios: Dr. Benjamin Clausen y Dra. Ana María Martínez Ardila**

**Monterrey, Nuevo León, México  
00 de mayo de 2021**

### **Abstract**

The classification of different rocks can provide important information about the conditions under they were formed and their tectonic environment. Color is a key property for rock classification. However, it is difficult to describe **color** in rocks because the perceived colors depend on the observer's experience. Moreover, the equipment for rock classification is expensive, which makes this equipment prohibitive to geology students and amateurs. The contribution of this research work is fourfold. First, since color is a key property for rock classification, feature reduction was applied to several patches of plutonic rock images extracting just their four dominant colors by means of the k-means clustering method. Second, different machine learning models were created and evaluated by means of applying the Logistic Regression (LR), K-Nearest Neighbors (KNN), Decision Trees (DT), Support Vector Machine (SVM), and a Convolutional Neural Network (CNN) algorithms to a dataset with the extracted dominant colors. The best results were achieved with **KNN** ~~that were the following:~~ 93% of accuracy, 93% of precision, 93% of recall, and 93% of F1-score. Third, we present an iOS application that uses **machine learning** to classify images of the following plutonic rocks: granite, granodiorite, gabbro, and diorite. The **results** of the iOS mobile application in the field were: 85.7% for granite, 20% for granodiorite, 70% for gabbro, and 28.5% for diorite. Four, we compared the results in the field with our previous work in which a CNN was trained using all the images features of the same dataset of plutonic rocks and deployed in an Android application.

### **Index Terms**

Machine Learning, Color Extraction, iOS Devices, Geology, Rock Classification, Features Reduction, Dominant Colors, K-means Clustering, Logistic Regression, K-Nearest Neighbors, Support Vector Machine, Convolutional Neural Network, Decision Trees.

## CONTENTS

<b>I</b>	<b>Introduction</b>	<b>1</b>
I-A	Background . . . . .	1
I-B	Problem Statement . . . . .	1
I-C	Justification . . . . .	1
I-D	Objectives . . . . .	1
I-E	Hypothesis . . . . .	2
<b>II</b>	<b>Theoretical Foundation</b>	<b>2</b>
II-A	Underpinnings of our Approach . . . . .	2
II-A1	Plutonic rocks . . . . .	2
II-A2	Machine Learning . . . . .	2
II-A3	Dominant colors . . . . .	3
II-A4	Underlying technologies . . . . .	3
II-B	Related Work . . . . .	3
II-B1	Image classification of rock lithology using machine learning . . . . .	4
II-B2	Rock classification with machine learning on Android devices . . . . .	4
II-B3	Recognition of mineral images applying machine learning and feature extraction . . . . .	4
II-B4	Discussion . . . . .	5
<b>III</b>	<b>Results</b>	<b>6</b>
III-A	Methodology . . . . .	6
III-A1	Getting the images of the plutonic rocks . . . . .	6
III-A2	Preparing the data . . . . .	6
III-A3	Determining the best number of color clusters . . . . .	6
III-A4	Color extraction . . . . .	6
III-A5	Data normalization and label encoding . . . . .	7
III-A6	Training the different algorithms with the extracted dominant colors . . . . .	7
III-A7	Evaluation of the machine learning algorithms . . . . .	8
III-B	Results . . . . .	9
III-C	Discussion . . . . .	9
<b>IV</b>	<b>Conclusions and Future Work</b>	<b>10</b>
	<b>References</b>	<b>10</b>

# Automatic classification of plutonic rocks with machine learning applied to extracted colors on iOS devices

Sarah Hernández, Germán H. Alférez, Benjamin Clausen and Ana M. Martínez

*School of Engineering and Technology, Montemorelos University, Mexico*

## I. INTRODUCTION

### A. Background

The classification of different rocks can provide important information about the conditions under which they were formed. They can also tell us much about their tectonic environment, given that they are closely linked to the convection of tectonic plates. Also, their mineral and chemical makeup can be used to learn about the composition, temperature and pressure that exists within the Earth's mantle [1].

Plutonic rocks are a type of igneous rock (one of the three main types of rocks in the world and also the most common) formed when magma in the middle of the volcanoes cools and solidifies below the Earth's surface. They come in many different sizes and colors, and have a wide variety of uses [2, 3].

Our contribution is fourfold. First we extracted the dominant colors of plutonic rock images grouping the image pixels according to their color in the RGB (Red, Green, Blue) and CIELab ( $L^*a^*b^*$ ) color spaces with the k-means algorithm. Color changes in rocks may indicate changes in the rock's mineral assemblage, texture, organic carbon content (shales), or other properties [4]. That is why color is a key property for rock classification. Second, we used the data of the dominant colors to create and evaluate several machine learning models with the following algorithms: Logistic Regression (LR), K-Nearest Neighbors (KNN), Decision Trees (DT), Support Vector Machine (SVM), and a Convolutional Neural Network (CNN). Third, we deployed the best model in an iOS application that classifies extracted colors in images into four types of plutonic rocks: granite, granodiorite, gabbro, and diorite. Fourth, we compare our approach with our previous work [reference] in which a CNN was trained with the same dataset of plutonic rock using the whole set of image pixel features instead of the four dominant colors. In that work, the

best result was obtained in the model that classifies images of gabbro, diorite, granodiorite, and granite with an accuracy value of 95%, an average precision of 96%, an average recall of 95%, and an average F1 score of 95%. Also, an Android mobile application was deployed with this classification model which results for diorite and granite were below expectations with 28.5% for each class.

### B. Problem Statement

The equipment for rock classification is expensive, which makes it prohibitive to geology students and amateurs. In addition, there is a lack of mobile tools for plutonic rock classification with machine learning. Despite the fact that color is a key property for rock classification, it is an attribute difficult to describe because perceived colors in rocks also depend on the observer's experience with similar observations; so a color may often be named differently by different persons [4].

### C. Justification

There are two reasons to create an iOS mobile application that allows the classification of plutonic rocks with machine learning using their dominant colors which represent the principal color values of all the pixels in an image. First, no such application exists. A mobile application offers the flexibility to carry out the classification on real time and could be an alternative to expensive traditional methods of rock classification. Second, in our previous work we found that the accuracy of the model decreased in the field. We extracted the dominant colors to verify if feature reduction leads to better results in the field than the obtained with the Android application of our previous work using all the rock image features.

### D. Objectives

The main objective of this research is to extract dominant colors from plutonic rock images to train several machine learning algorithms and deploy the best model in an iOS app. In this way we will be able to compare the results in the field with our previous work. This objective is achieved with the following sub-objectives:

- Determine the best k number of clusters to use in the k-means clustering machine learning method to extract the dominant colors from images of plutonic rocks.

Sarah Hernández is a computer science engineering student at the School of Engineering and Technology of Montemorelos University, Nuevo León, Mexico, e-mail: 1170469@alumno.um.edu.mx.

Germán H. Alférez, Ph.D., is the director of the Institute of Data Science and professor at the School of Engineering and Technology of Montemorelos University, Nuevo León, Mexico, e-mail: harveyalferez@um.edu.mx.

Benjamin Clausen, Ph.D., is a professor at the Department of Earth and Biological Sciences of Loma Linda University, California, USA, e-mail: bclausen@llu.edu.

Ana M. Martínez, Ph.D., is a professor at the Department of Earth and Biological Sciences of Loma Linda University, California, USA, e-mail: anmartinez@llu.edu.

- Use the extracted dominant colors and the percentage of pixels belonging to each color cluster as the input to train the following machine learning algorithms: LR, KNN, DT, SVM, and a CNN.
- Validate the models generated to get the best suited model and deploy it in an iOS mobile application.
- Test the effectiveness of the application with images taken from new plutonic rocks to compare the results with our previous work in which a CNN was trained with images using the whole set of features.

### E. Hypothesis

The training of a machine learning model with just the dominant colors extracted from granite, granodiorite, gabbro, and diorite images can provide an effective way for the classification of these plutonic rocks.

## II. THEORETICAL FOUNDATION

### A. Underpinnings of our Approach

Our approach is based on the following concepts (see Fig. 1).

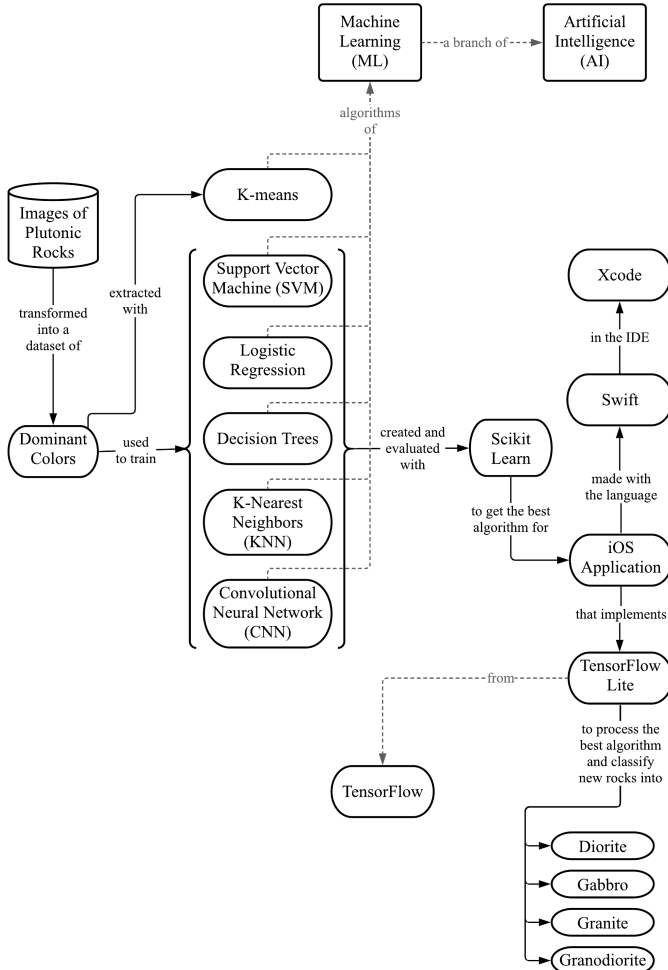


Figure 1. Underpinnings of our approach

### 1) Plutonic rocks

Plutonic rocks are solidified inside the earth's crust, usually from magma, although they may have been formed by a different mechanism. Plutonic rocks are generally coarse-grained, but not all coarse-grained rocks are plutonic [5].

According to [5]:

Granite rocks are plutonic rocks with a granular texture, composed of similar amounts of quartz, potassium feldspar, and plagioclase as essential minerals, and smaller amounts of one or more minerals, such as biotite, muscovite or hornblende.

Granodiorite is a plutonic rock of the granitoid family, characterized by quartz because plagioclase constitutes more than 2/3 of the total feldspars. Generally, together with granite, it is the most abundant rock of the great batholiths. Its volcanic equivalent is dacite. Granodiorite is similar to granite, but with less potassium feldspar and more plagioclase.

Gabbro is a plutonic rock composed mainly of calcium plagioclase and clinopyroxene or orthopyroxene, with or without olivine or amphibole. It is the intrusive equivalent of basalt. It is distinguished from diorite by the nature of plagioclase, which is higher in calcium than in sodium.

Diorite has about the same structural properties as granite but darker colour and more limited supply. Commonly is composed of about two-thirds plagioclase feldspar and one-third dark-coloured minerals, such as hornblende or biotite. The presence of sodium-rich feldspar, oligoclase or andesine, in contrast to calcium-rich plagioclase, labradorite or bytownite, is the main distinction between diorite and gabbro [6].

### 2) Machine Learning

Machine learning is a branch of artificial intelligence that lies at the intersection of computer science, engineering and statistics, and often appears in other disciplines. Machine Learning systems can be classified according to the type of supervision they get during training [7, 8]. In this way, there are two major categories:

#### a) Supervised learning

In supervised learning, the training set fed to the algorithm includes the desired solutions, called labels. A typical supervised learning task is classification [8].

Some common algorithms of supervised learning are described as follows:

- Logistic Regression (LR) is commonly used to estimate the probability of an instance to belong to a particular class. This model computes a weighted sum of the input features (plus a bias term) and outputs the logistic of this result. The logistic is a sigmoid function that outputs a number between 0 and 1. This makes it a binary classifier [8].
- K-Nearest Neighbors (KNN) is a simple algorithm in which its principle is to find a predefined number of training samples closest in distance to the new point, and predict the label from these. Being a non-parametric method, it is often successful in classification situations where the decision boundary is very irregular [9].
- Decision Trees (DT) algorithm consists of split nodes and leaf nodes. Each split node performs a split decision

and routes a data sample either to the left or the right child node. In the tree structures, leaves represent the labels, non-leaf nodes are the input features, and branches represent conjunctions of features that lead to the classifications [10, 11].

- Support Vector Machine (SVM) algorithm is a powerful and versatile machine learning model, particularly well suited for classification of complex small- or medium-sized datasets. In this algorithm, the data is plotted in a  $n$ -dimensional space (number of features) and a decision boundary (hyperplane) split it into classes [8, 7].
- Convolutional Neural Networks (CNNs) emerged from the study of the brain's visual cortex. The most important building block is the convolutional layer. The CNN's architecture consists of several connected layers allowing the network to concentrate on small low-level features in the first hidden layer, then assemble them into larger higher-level features in the next layer, and so on [8].

#### *b) Unsupervised learning*

In unsupervised learning the training data is unlabeled. One of the most important unsupervised learning algorithms is  $k$ -means.  $K$ -means is a simple algorithm capable of clustering an unlabeled dataset very quickly and efficiently, often in just a few iterations. The number of clusters  $k$  that the algorithm must find is specified to easily label all the instances in the dataset by assigning each of them to the cluster whose centroid is closest [8].

#### *3) Dominant colors*

The dominant colors refer to the principal colors presented in an image. The dominant colors of an image are selected grouping the image pixels according to their color in the selected color space (RGB and CIELab). The average color of each group are the dominant colors and the number of pixels of that groups are the percentage of the dominant colors.

In RGB (Red, Green, Blue), the light spectra of varying fractions of the three primary colors referred to as channels, combine to make new colors. Each channel has intensity values from 0 to 1 that are scaled by the number of bits used to represent each component. The 24-bit color cube used in this research has components in the range of 0–255. Each color in the color space can be represented as a three-value vector [12].

#### *4) Underlying technologies*

##### *a) Scikit learn*

Scikit-learn is a Python module that integrates a wide range of state-of-the-art machine learning algorithms for medium-scale supervised and unsupervised problems. This package focuses on bringing machine learning to non-specialists using a general-purpose high-level language. Emphasis is put on ease of use, performance, documentation, and API consistency. It has minimal dependencies and is distributed under the simplified Berkeley Source Distribution (BSD) license, encouraging its use in both academic and commercial settings [13].

##### *b) Tensorflow*

TensorFlow<sup>1</sup> is an open-source library developed by Google. It has become very popular because it provides Application Programming Interfaces (APIs) that facilitates machine learning. TensorFlow also has a faster compilation time than other deep learning libraries such as Keras and Touch. TensorFlow supports both CPU and GPU computing devices [14].

##### *c) Tensorflow Lite*

TensorFlow Lite<sup>2</sup> is a set of tools to help developers run TensorFlow models on mobile, embedded, and IoT devices. It enables on-device machine learning inference with low latency and a small binary size [15].

TensorFlow Lite consists of two main components:

- The TensorFlow Lite interpreter, which runs specially optimized models on many different hardware types, including mobile phones, embedded Linux devices, and microcontrollers.
- The TensorFlow Lite converter, which converts TensorFlow models into an efficient form for use by the interpreter, and can introduce optimizations to improve binary size and performance.

##### *d) Swift*

Swift<sup>3</sup> is an open source programming language designed for macOS, iOS, watchOS, tvOS, and more. Swift already supports all Apple platforms and Linux, with community members actively working to port to even more platforms [16]. In 2010, Apple started developing Swift, a new programming language that would rival Objective-C in type safety, security, and hardware performance. Swift is more than 2.6x faster than Objective-C and more than 8.4x faster than Python [17].

##### *e) Xcode*

Xcode<sup>4</sup> is a long-standing tool for app production and a well-known integrated development environment (IDE), enabling developers to write the code and compile apps that can be used on a variety of different devices and operating systems [18]. It also includes a unified macOS SDK and all the frameworks, compilers, debuggers, and other tools necessary to build applications that run natively on Apple devices [19].

##### *f) CocoaPods*

CocoaPods<sup>5</sup> is a dependency manager for Swift and Objective-C Cocoa projects. The dependencies of the projects just are specified in a single text file called Podfile. CocoaPods resolves dependencies between libraries, fetches the resulting source code, then links it together in an Xcode workspace to build a single project [20].

#### *B. Related Work*

Over the last decade, there has been considerable progress in the application of machine learning to geosciences [21]. In this section we present relevant research work in three areas: image classification of rock lithology using machine learning, rock classification with machine learning on Android devices,

<sup>1</sup><https://www.tensorflow.org>

<sup>2</sup><https://www.tensorflow.org/lite>

<sup>3</sup><https://swift.org>

<sup>4</sup><https://developer.apple.com/xcode/>

<sup>5</sup><https://cocoapods.org>

and recognition of mineral images applying machine learning and feature extraction.

### 1) *Image classification of rock lithology using machine learning*

In [22], Ran et al. proposed a CNN model for the classification of six rock types (granite, limestone, conglomerate, sandstone, shale, mylonite) and compared their results with four other common machine learning models. A total of 2,290 images were labeled according to the clarity of the rock and cropped into 14,589 sample patches of  $512 \times 512$  pixels compressed to  $128 \times 128$  pixels. 60% of the patches of each type of rock were selected for the training dataset, 20% for the validation dataset, and 20% for the testing dataset. Their proposed CNN model achieved the highest overall accuracy of 97.76% compared with the other models: SVM, AlexNet, GoogleLeNet Inception v3, and VGGNet-16.

In [23], Cheng and Guo proposed a deep CNN to identify the granularity of feldspar sandstone rocks in images under three color spaces: RGB, YCbCr, and HSV. A total of 4,200 images were collected from rocks of an oil field in Ordos and divided into three types of granularity: coarse, medium granular, and fine. The RGB images were normalized to  $224 \times 224$  pixels and converted to YCbCr and HSV. The proposed CNN was a 6-layer structure of 4 convoluted layers with ReLU as the activation function and 2 fully connected layers with Softmax as the classifier. The model was trained for each color space with 75% of the experimental data, a batch size of 100, and different kernel sizes and learning rates. The lowest error rates were obtained with the learning rate of 0.0005, the kernel sizes of 11, 5, 3, and 3 for each convolutional layer respectively, and the cross-validation for HSV color space. In RGB color space, the classification accuracy achieved 98.5%.

### 2) *Rock classification with machine learning on Android devices*

In [24], Fan et al. created a method for rock lithology recognition on Android devices based on the two lightweight SqueezeNet and MobileNet CNNs. These models were compared with ResNet50, a heavyweight model. The images were selected from the China Geological Survey dataset that contains images of 28 rock categories taken by a smartphone camera. The 3,208 images were reduced to  $214 \times 214$  pixels and the 80% were used to train the two CNNs pretrained with ImageNet dataset. The achieved occupation sizes were 19.6 M and 36.8 M for MobileNet and SqueezeNet, and 232.7 M for ResNet50. SqueezeNet was almost two times faster than MobileNet, and 7 times faster than ResNet50. A rock recognition software based on the trained models was developed for Android devices. The results for SqueezeNet and MobileNet on Android smartphones were as follows: the file sizes of 9.2 MB and 17.6 MB, the execution time from 736 to 366 and 1,218 to 523 milliseconds, and the recognition accuracies of 94.55% and 93.27%.

Also in [25], Fan et al. improved their work using a model based on ShuffleNet for quick and accurate rock lithology recognition with smartphones and compared it with their previous work of MobileNet and SqueezeNet. They selected 3,795 images of 30 different kinds of rocks collected from multiple

locations in East China. The ShuffleNet model was trained using 80% of the dataset, 3,600 iteration steps, a learning rate of 0.008, and the parameters imported by the transfer learning method using the ImageNet dataset. ShuffleNet occupied a space of 18.2M compared with MobileNet, SqueezeNet, and ResNet50 that occupied 34.5M, 25M, and 219.4M respectively. An Android application was created using each model and run on three Android smartphones (Huawei, Samsung, and Oppo). The average recognition time of ShuffleNet for a single rock image was 786 milliseconds, the reached accuracy was 97.65% on PC and 95.30% on the smartphones.

In our previous work [], we proposed a CNN model trained with several combinations of plutonic rocks to deploy the best combination of rocks in an Android application. The dataset contained 71 images of diorite, gabbro, granite, granodiorite, monzodiorite, and tonalite which classification was based on petrographic analysis of Cretaceous granitoids collected from Peru. To increase the number of images, a new dataset of 846 patches from around  $450 \times 700$  to  $900 \times 1000$  pixels was generated from the first dataset. A deep neural network was created with 4-layer structure: two convolutional, and two fully connected layers. After each convolutional layer it was a max pooling layer of  $2 \times 2$  size, and a flatten and a dropout layers before the first and second fully connected layers respectively. Several combinations of the rock classes were trained with 50% of the image patches, 100 epochs and a batch size of 32. The best combination was with four classes of plutonic rocks (gabbro, diorite, granite and granodiorite) achieving an accuracy of 95%, an average precision of 96%, an average recall of 95%, and an average F1-score of 95%. Finally, an Android application was developed using the proposed model trained with the best combination of rocks. The application evaluation results were: 70% for gabbro, 28.5% for diorite, 100% for granodiorite, and 28.5% for granite.

### 3) *Recognition of mineral images applying machine learning and feature extraction*

In [26], Zhang et al. worked on the intelligent identification for rock-mineral images using ensemble machine learning algorithms (model stacking). A total of 481 images of four minerals (K-feldspar, perthite, plagioclase, and quartz) were obtained with the camera on the top of a microscope. The target RGB images were cropped to cover the minerals and then processed to be  $299 \times 299$  pixels. A deep learning model based on Inception-v3 was adopted to extract high-level features (such as chromatic aberration and texture) from the images and train the algorithms of LR, SVM, KNN, Random Forest (RF), Multilayer Perceptron (MLP), and Gaussian Naive Bayes (GNB). LR, SVM, and MLP had a significant effect on extracted features, with higher accuracy (90.0%, 90.6%, and 89.8%) than the other models. The new features generated by this three models were employed for the model stacking in a new instance of LR. The stacking model showed a better performance than the single models, with an accuracy of 90.9%.

In [27], Maitre et al. created several models of supervised machine learning to recognize mineral grains in a sample surface containing grains of 27 different mineral species (pla-

Table I  
COMPARISON TABLE OF THE ARTICLES DESCRIBED IN THE RELATED WORK

Author	Year	Dataset	Algorithm of extraction	Extracted features	Dataset for training	Best trained model	Results
Zhang et al. [26]	2019	481 images of four minerals (K-feldspar, perthite, plagioclase, and quartz)	Inception-v3 CNN model	High-level features (such as chromatic aberration and texture)	90% of extracted features	Stacking model (LR, SVM, and MLP)	Model accuracy: 90.9% -
Maitre et al. [27]	2019	3,192 sub-images of the view taken to a surface with 27 mineral grains species	Simple Linear Iterative Clustering (SLIC) algorithm	Color intensity and Peak intensity of computed histograms from superpixels	70% of extracted features	Random Forest (RF)	Model accuracy: 89% -
Ran et al. [22]	2019	14,589 patches from 2,290 images of six rock types (granite, limestone, conglomerate, sandstone, shale, mylonite)	-	-	60% of the patches	3-layer structure CNN	Model accuracy: 97.76% -
Cheng and Guo [23]	2017	4,200 images of three feldspar sandstones rock types (coarse, medium granular, and fine)	-	-	75% of the images	6-layer structure CNN	Model accuracy: 98.5% -
Fan et al. [24]	2020	3,208 images of 28 rock lithology categories	-	-	80% of the images	SqueezeNet and MobileNet	Android application accuracies: 94.55% and 93.27% File sizes: 9.2 MB and 17.6 MB Execution times: 736 to 366 and 1,218 to 523 millisecond
Fan et al. [25]	2020	3,795 images of 30 different rock types	-	-	80% of the images	ShuffleNet	Android application accuracy: 97.65% Occupation space on PC: 18.2M Classification time: 786 millisecond
E. Vázquez and H. Alférez []	2021	846 patches from 71 images of six plutonic rock types (diorite, gabbro, granite, granodiorite, monzodiorite, and tonalite)	-	-	50% of the patches	4-layer structure CNN	Model accuracy: 95% Android application accuracy results: 70% for gabbro, 28.5% for diorite, 100% for granodiorite, and 28.5% for granite

gioclase, augite, background, hypersthene, ilmenite, magnetite, titanite, hornblende, etc.). The surface was scanned with an automated Scanning Electron Microscopy (SEM) that assigned to each grain a mineral specie based on its chemical signature. Also several views of the same surface were taken with a stereo-zoom binocular microscope to construct a large mosaic RGB image. Both images were divided in 3,192 sub-images of  $600 \times 600$  pixels. To label the grains of the mosaic image, the simple linear iterative clustering (SLIC) algorithm was applied for superpixel segmentation to match each superpixel of the mosaic's sub-images with the superpixels of the SEM's scan sub-images. From the computed RGB superpixel histograms, the color intensity (quantile) and peak intensity (ratio between the number of pixels in the first and second maximum bins to total number of pixels) were extracted as features for each superpixels. KNN, RF, and Classification and Regression Trees

(CART) algorithms were trained with 70% of the extracted features, and tested with the other 30% using the kappa statistics, precision, recall, and f1-score indicators. The RF algorithm gave the best results with a global accuracy of 89%.

#### 4) Discussion

Table I illustrates the comparison of the articles described in this section. As evidenced in these articles, machine learning has been an effective way for image classification in geochemistry and geosciences.

Feature extraction was applied in [27] and [26] before the training of several machine learning models to classify images of mineral samples. These works showed higher accuracies from around 90% but the number of extracted features per instance used for training was even too large compared with the 16 features used in this work.



Four articles [22, 23, 24, 25] introduced the comparison of different CNN model structures to analyze the performance of these models for rock lithology classification using all the image features. Also in our previous work [reference], several combinations of plutonic rocks were analyzed using all the image features to train a CNN model rather than extracted features. In [24, 25] and [reference] the created models were implemented on android mobile applications for the classification of rocks. However there are no works presenting the evaluation results of the deployment of machine learning on iOS devices.

The evaluation of the models in [22, 23, 24, 25] showed great results, though all of them were trained with diverse types of rocks instead of on type as was made in this work classifying just plutonic rocks. This type of classification becomes more difficult because rocks of a same type have very similar characteristics.

### III. RESULTS

#### A. Methodology

This section describes the steps followed in this research work.

##### 1) Getting the images of the plutonic rocks

The images of plutonic rocks were provided by the Department of Earth and Biological Sciences at Loma Linda University. The dataset contains images of four classes of plutonic rocks: granite, granodiorite, gabbro, and diorite with a total of 81 images. The images used in the following experiments are available online<sup>6</sup>. Table II shows the number of images per class.

Table II  
NUMBER OF IMAGES PER CLASS

Class	Number of images
Granite	16
Granodiorite	21
Gabbro	19
Diorite	25
<b>Total of images</b>	<b>81</b>

##### 2) Preparing the data

In this step, the images were processed in order to obtain the color values of the image pixels in RGB and CIELab color spaces.

First, all files with image extension ('.png', '.jpg', '.jpeg') in the main directory of images were processed in RGB format and labeled according to the name of the subfolder containing each one. Thereafter, we converted the RGB values of the image pixels to CIELab values using the "rgb2lab" function of the color class of Scikit-image module. In this way, we can train the models in the two color spaces. The notebook with the source code for data preparation is available online<sup>7</sup>

<sup>6</sup><https://github.com/sarah-hs/Color-extraction/tree/main/Rock-images>

<sup>7</sup><http://bit.ly/3pyh3JL>

##### 3) Determining the best number of color clusters

The k-means algorithm is used to extract the dominant colors from the images. The Elbow method was used to calculate the optimal number of clusters to use in k-means. This method consists of iterating in a range of possible cluster numbers and determine the best one. We declared the range of 2 to 20 to obtain the scores of k-means trained with each cluster number and the pixel values of a sample image. These scores were plotted with their respective k numbers. The number at the elbow of the plot is the best k number of clusters which is 4 for this experiment (see Fig. 2).

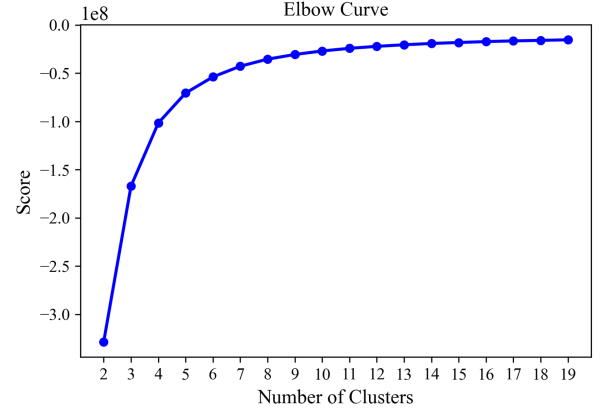


Figure 2. The Elbow method showing the optimal k number of clusters

##### 4) Color extraction

This step describes the process for extracting the dominant colors from the rock images. In listing 1, the "get\_dominant\_colors" function receives the pixel values of an image to train the k-means algorithm with 4 clusters, which is the number of clusters selected in the previous step. In line 6, k-means works by separating the pixels of that image into k groups (clusters) of similarly coloured pixels. The colors at each cluster center reflect the average of the attributes of all members of a cluster. The percentage of a cluster calculated in lines 8 to 10 is the number of pixels within that cluster. From lines 14 to 18, the center color in each cluster and its percentage is added to the features list returned in line 20. This list has sixteen elements: the four main colors represented by the three channels of the selected color format and the percentage of each dominant color (see Fig. 3).

```

1 from sklearn.cluster import KMeans
2 CLUSTERS = 4
3
4 def get_dominant_colors(img):
5     reshape = img.reshape((img.shape[0] * img.shape[1],
6                             img.shape[2]))
7     cluster = KMeans(n_clusters=CLUSTERS).fit(reshape)
8     labels = np.arange(0,
9                       len(np.unique(cluster.labels_)) + 1)
10    (hist, _) = np.histogram(cluster.labels_, bins =
11                             labels)
12    hist = hist.astype("float"); hist /= hist.sum()
13
14    features = []
15
16    colors = sorted([(percent, color) for (percent,
17                                         color) in zip(hist, cluster.cluster_centers_)])
18
19    for (percent, color) in colors:

```

```

17     features.extend(color)
18     features.append(percent)
19
20     return features

```

Listing 1. Function to extract the dominant colors from a single image

In listing 2, the processed data of the rock images is iterated to extract the dominant colors with the previous explained “get\_dominant\_colors” function of listing 4. These colors are added to a new array called “extracted\_colors”. In line 6, the extracted colors are saved together with their respective rock label in a CSV file. This file is used in the next step to train the machine learning algorithms. The CSV is available online<sup>8</sup>.

```

1  extracted_colors = []
2  for img in images:
3      features = get_dominant_colors(img)
4      extracted_colors.append(features)
5
6  data_df = pd.DataFrame(extracted_colors, files)
7  data_df[16] = y
8  data_df.to_csv(CSV_DIR, header=None)

```

Listing 2. Iterate original data to extract dominant colors

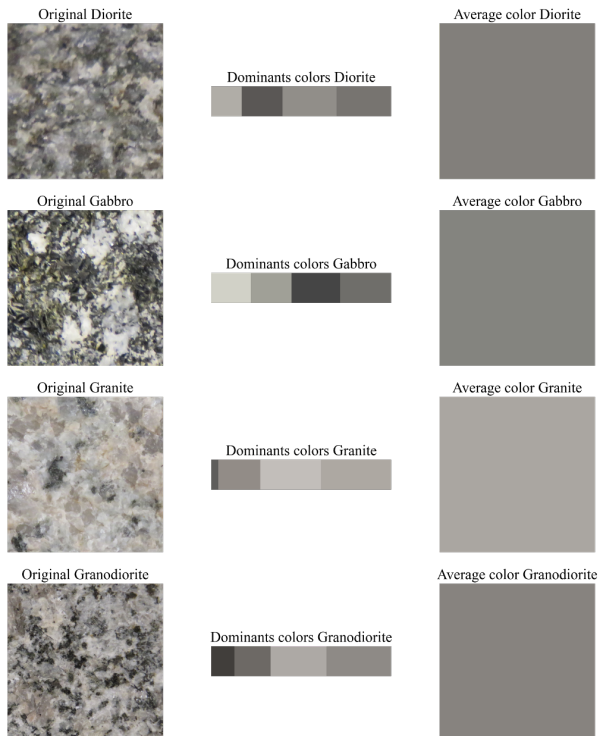


Figure 3. Dominant colors and average color of sample images

### 5) Data normalization and label encoding

First, in this step we loaded the extracted colors data from the CSV of the pixel values into x and y. Second, in order to train and test the models, the data was splitted into a training set of 80% and a testing set of 20%. The extracted feature values were normalized scaling each feature to a given range of 0 to 1 and the labels were converted to number data with the “train\_test\_split” and the “LabelEncoder” functions of the model\_selection class from scikit-learn module respectively.

Data normalization is useful to clean the data and obtain better results in model training.

### 6) Training the different algorithms with the extracted dominant colors

Five machine learning models were trained for this experiment: LR, KNN, DT, SVM, and a CNN. The notebook showing the training and validation process of the generated models is available online<sup>9</sup>.

Below, listings 3-7 present the set and training process of the models. Three models (LR, KNN, and CNN) were trained with the normalized data while the others (DT and SVM) with non-normalized data. The following configurations were used to set the models:

LR was set in line 3 of listing 3 with the L-BFGS (Limited-memory Broyden–Fletcher–Goldfarb–Shanno) solver which is one of the quasi-Newton methods that approximate the BFGS algorithm, which utilizes a limited amount of computer memory. The solver’s methodology starts iterating at a random point (xt) to calculate the minimum from the second derivate of the original function at that point and assign it to a new point (xt+1). The new point will become the starting point for the next iteration. In this way, L-BFGS quickly converges on the solution [28].

```

1  # Logistic Regression
2  from sklearn.linear_model import LogisticRegression
3  logReg = LogisticRegression(solver='lbfgs')
4  logReg.fit(xtrainNorm, ytrain)

```

Listing 3. Set and training of LR

The number of neighbors used for KNN in line 3 of listing 4 represents the neighbor samples analyzed from the dataset to classify a new sample into the class to which most of their neighbors belong.

```

1  # K-Nearest Neighbors
2  from sklearn.neighbors import KNeighborsClassifier
3  knn = KNeighborsClassifier(n_neighbors=1)
4  knn.fit(xtrainNorm, ytrain)

```

Listing 4. Set and training of KNN

By utilizing class weights, we can increase the importance of a particular class during training. DT is set in line 3 of listing 5 with the balanced mode for class weight that uses the label values of the training set to automatically adjust the node weights inversely proportional to the class frequencies in the input data [28].

```

1  # Decision Trees
2  from sklearn.tree import DecisionTreeClassifier
3  decisionTree =
4      DecisionTreeClassifier(class_weight='balanced')
5  decisionTree.fit(xtrain, ytrain)

```

Listing 5. Set and training of DT

SVM is set in line 3 of listing 6 with the Radial Basis Function (RBF) kernel, useful to eliminate the computational requirement of an algorithm. When it is used, the features need to be scaled and the gamma value is setting for. The auto value represents gamma by  $1/\text{numberOfFeatures}$ . An small

<sup>8</sup><https://github.com/sarah-hs/Color-extraction/blob/main/colors.csv>

<sup>9</sup><https://github.com/sarah-hs/Color-extraction/blob/main/ML-training.ipynb>

gamma will give you low bias and high variance solutions [28, 29].

```
1 # Support Vector Machines
2 from sklearn.svm import SVC
3 svmc = SVC(kernel='rbf', gamma='auto')
4 svmc.fit(xtrain, ytrain)
```

Listing 6. Set and training of SVM

Table III describes the structure of the CNN model set in lines 7-14 of listing 7.

Table III  
CNN MODEL STRUCTURE

Layer	Filters	Kernel size	Activation function	Output shape
Input features	-	-	-	16
Conv1D	32	2	RELU	16 × 32
MaxPooling1D	-	2	-	8 × 32
Conv1D	64	2	RELU	8 × 64
MaxPooling1D	-	2	-	4 × 64
Flatten	-	-	-	256
Dense	64	-	RELU	64
Dense	4	-	Softmax	4

The CNN was compiled in line 15 with the categorical crossentropy loss function and the Adam optimizer. Categorical cross-entropy is the most diffused classification cost function, adopted by logistic regression and the majority of neural architectures. This convex function can be easily optimized using stochastic gradient descent techniques and is an excellent choice for classification problems [30]. In the other hand, Adam (adaptive moment estimation) algorithm is an efficient optimization method that computes adaptive learning rates for each parameter to optimize the weights of the model [28]. Finally, to train CNN several numbers of epochs and batches were tried until the most optimal values were obtained as shown in line 19.

```
1 # Convolutional Neural Network
2 from tensorflow.keras.models import Sequential
3 from tensorflow.keras.layers import Dense, Flatten,
4 Dropout, Conv1D, MaxPooling1D
5 from tensorflow.keras import optimizers
6 from livelossplot.inputs.tf_keras import
7 PlotLossesCallback
8
9 model = Sequential()
10 model.add(Conv1D(32, kernel_size=2, padding="same",
11 input_shape = (16, 1), activation='relu'))
12 model.add(MaxPooling1D(pool_size=2))
13 model.add(Conv1D(64, kernel_size=2, padding="same",
14 activation='relu'))
15 model.add(MaxPooling1D(pool_size=2))
16 model.add(Flatten())
17 model.add(Dense(64, activation='relu'))
18 model.add(Dense(16, activation='softmax'))
19 model.compile(loss='sparse_categorical_crossentropy',
20 optimizer='adam', metrics=['accuracy'])
21
22 xtrain2 = np.expand_dims(xtrainNorm, 2)
23 ytrain2 = np.expand_dims(ytrain, 1)
24 model.fit(xtrain2, ytrain2, epochs=100, batch_size=32)
```

Listing 7. Set and training of CNN

## 7) Evaluation of the machine learning algorithms

Evaluating a model is a core part of building an effective machine learning project. For this purpose are used the following four metrics to evaluate the algorithms [31]:

- Accuracy is the ratio of number of correct predictions to the total number of input samples.

$$Accuracy = \frac{CorrectPredictions}{PredictionsMade}$$

- Precision is the number of correct positive results divided by the number of positive results predicted by the classifier.

$$Precision = \frac{TP}{TP + FP}$$

- Recall is the number of correct positive results divided by the number of all relevant samples (all samples that should have been identified as positive).

$$Recall = \frac{TP}{TP + FN}$$

- F1-score is used to measure a test's accuracy, the Harmonic Mean between precision and recall. It tells you how precise your classifier is (how many instances it classifies correctly), as well as how robust it is (it does not miss a significant number of instances).

$$F1 = 2 * \frac{Precision * Recall}{Precision + Recall}$$

The greater the F1-score, the better is the performance of our model.

Table IV shows the accuracy of all the trained algorithms evaluated with the test set of the previous step.

Table IV  
RESULTS OF ALL THE ALGORITHMS IN TERMS OF ACCURACY

Model	Accuracy
Logistic Regression	0.63
KNN	0.93
Decision Trees	0.72
SVM	0.80
CNN	0.82

Tables V-IX show the results of each model evaluation in terms of precision, recall and F1-score. The best results were obtained with the KNN model with the highest average values of 93% for accuracy, 93% for precision, 93% for recall, and 93% for f1-score.

Table V  
RESULTS OF LOGISTIC REGRESSION

Class	Precision	Recall	F1-score
Granite	0.81	1.00	0.90
Granodiorite	0.64	0.50	0.56
Gabbro	0.50	0.77	0.61
Diorite	0.60	0.35	0.44
Average	0.64	0.66	0.63

Table VI  
RESULTS OF K-NEAREST NEIGHBORS

Class	Precision	Recall	F1-score
Granite	1.00	0.92	0.96
Granodiorite	0.92	0.79	0.85
Gabbro	0.93	1.00	0.96
Diorite	0.89	1.00	0.94
<b>Average</b>	<b>0.93</b>	<b>0.93</b>	<b>0.93</b>

Table VII  
RESULTS OF DECISION TREES

Class	Precision	Recall	F1-score
Granite	0.86	0.92	0.89
Granodiorite	0.73	0.57	0.64
Gabbro	0.56	0.69	0.62
Diorite	0.75	0.71	0.73
<b>Average</b>	<b>0.72</b>	<b>0.72</b>	<b>0.72</b>

Table VIII  
RESULTS OF SUPPORT VECTOR MACHINE

Class	Precision	Recall	F1-score
Granite	0.87	1.00	0.93
Granodiorite	0.80	0.57	0.67
Gabbro	0.68	1.00	0.81
Diorite	0.92	0.71	0.80
<b>Average</b>	<b>0.82</b>	<b>0.82</b>	<b>0.80</b>

Table IX  
RESULTS OF THE CONVOLUTIONAL NEURAL NETWORK

Class	Precision	Recall	F1-score
Granite	0.93	1.00	0.96
Granodiorite	0.67	0.57	0.62
Gabbro	0.81	1.00	0.90
Diorite	0.87	0.76	0.81
<b>Average</b>	<b>0.82</b>	<b>0.83</b>	<b>0.82</b>

## B. Results

The KNN model was the model deployed in the iOS mobile application to make the classification on real-time. The Xcode IDE, the Xcode command-line tools, a valid Apple Developer ID, and the CocoaPods dependency manager were the main requirements to develop it. The application is written mostly in Swift and uses the following two libraries for performing dominant colors extraction and image classification:

- The DominantColor<sup>10</sup> dependency is an open source library written in Swift and created by Indragie Karunaratne. It finds the dominant colors of an image using the CIE LAB color space and the k-means clustering algorithm. In this project an adaptation of this library was implemented exporting the 7 main files from the repository into the application project.
- The TensorFlow Lite Swift<sup>11</sup> library is TensorFlow's lightweight solution for Swift developers. It enables low-latency inference of on-device machine learning models

with a small binary size and fast performance supporting hardware acceleration. For the application, TensorFlow Lite Swift pod name was added into the project's Podfile, and from command line the library was resolved into the Xcode project by the CocoaPods dependency manager.

Shown below is the application process (see Fig. 4). The source code of the application is available online<sup>12</sup>.

## C. Discussion

Five machine learning algorithms were trained with just the four dominant colors extracted from rock images. The best algorithm in this experiment was K-Nearest Neighbors with an accuracy of 82%. Its values for precision, recall, and F1 score were 84%, 89%, and 83%. Table X presents the comparison of these results and the results of our previous approach with a CNN using all the image features.

Table X  
COMPARISON OF THE BEST MODELS IN THIS RESEARCH AND THE BEST MODEL PRESENTED IN OUR PREVIOUS WORK

Metrics	KNN of this work	CNN of our previous work
Accuracy	93%	95%
Precision	93%	96%
Recall	93%	95%
F1-score	93%	95%

After obtaining the best suited algorithm for rock classification with dominant colors, an iOS mobile application was developed to classify rock images into four classes of plutonic rocks (granite, granodiorite, gabbro and diorite). This application also allows the user to visualize the dominant colors and the average color in new images and detect changes in rock colors. The application was tested in the field and the following results were obtained: 85.7% for granite, 20% for granodiorite, 70% for gabbro, and 28.5% for diorite. As shown in table XI the results of diorite and gabbro were the same as the obtained in our previous work. The results of granodiorite were below expectations compared with our previous work. An improvement is observed in the results for granite with the dominant color approximation.

Table XI  
RESULTS COMPARISON OF THE iOS APPLICATION AND THE ANDROID APPLICATION OF OUR PREVIOUS WORK IN THE FIELD

Class	Total of images taken	Correctly classified in this work		Correctly classified in our previous work	
		Images	Percent	Images	Percent
Granite	7	6	85.7%	2	28.5%
Granodiorite	10	2	20%	10	100%
Gabbro	10	7	70%	7	70%
Diorite	7	2	28.5%	2	28.5%
<b>Total</b>	<b>34</b>	<b>17</b>	<b>50%</b>	<b>21</b>	<b>61%</b>

<sup>12</sup><https://github.com/sarah-hs/Rock-Classifer-iOS>

<sup>10</sup><https://github.com/indragiek/DominantColor>

<sup>11</sup><https://github.com/tensorflow/tensorflow/tree/master/tensorflow/lite/swift>

## IV. CONCLUSIONS AND FUTURE WORK

## REFERENCES

- [1] M. Williams, *Igneous rocks: How are they formed?* English, Access date: 12/16/2020, Universe Today, Dec. 2015. [Online]. Available: <https://www.universetoday.com/82009/how-are-igneous-rocks-formed/>.
- [2] National Geographic Society, *Igneous rocks*, English, ENCYCLOPEDIA ENTRY, Access date: 12/16/2020, National Geographic, Oct. 2019. [Online]. Available: <https://www.nationalgeographic.org/encyclopedia/igneous-rocks/>.
- [3] R. Gillaspay, *Volcanic vs plutonic igneous rocks: Definition and differences*, English, Access date: 12/16/2020, Study.com, Nov. 2013. [Online]. Available: <https://study.com/academy/lesson/volcanic-vs-plutonic-igneous-rocks-definition-and-differences.html>.
- [4] Natural Resources Conservation Service, “Part 631: Geology,” in *National Engineering Handbook*, 210-VI, Access date: 12/16/2020, 2012, ch. 4, p. 7. [Online]. Available: <https://directives.sc.egov.usda.gov/OpenNonWebContent.aspx?content=31848.wba>.
- [5] f. y. n., *RACEFEN Glosario de geología*, Spanish, Access date: 01/04/2021, España: Real academia de ciencias exactas, físicas y naturales. [Online]. Available: [http://www.ugr.es/~agcasco/personal/rac\\_geologia/0\\_rac.htm](http://www.ugr.es/~agcasco/personal/rac_geologia/0_rac.htm).
- [6] Encyclopædia Britannica, *Diorite*, English, Access date: 12/15/2020, Encyclopædia Britannica, Jan. 2009. [Online]. Available: <https://www.britannica.com/science/diorite>.
- [7] P. Harrington, *Machine Learning in Action*. MANNING PUBN, Apr. 1, 2012, 384 pp., ISBN: 1617290181. [Online]. Available: [https://www.ebook.de/de/product/15619827/peter\\_harrington\\_machine\\_learning\\_in\\_action.html](https://www.ebook.de/de/product/15619827/peter_harrington_machine_learning_in_action.html).
- [8] A. Géron, *Hands-on Machine Learning with Scikit-Learn, Keras, and TensorFlow*. O’Reilly UK Ltd., Oct. 1, 2019, 819 pp., ISBN: 1492032646. [Online]. Available: [https://www.ebook.de/de/product/33315532/aurelien\\_geron\\_hands\\_on\\_machine\\_learning\\_with\\_scikit\\_learn\\_keras\\_and\\_tensorflow.html](https://www.ebook.de/de/product/33315532/aurelien_geron_hands_on_machine_learning_with_scikit_learn_keras_and_tensorflow.html).
- [9] Scikit-learn, *Nearest Neighbors*, English, Access date: 12/15/2020, Scikit-learn. [Online]. Available: <https://scikit-learn.org/stable/modules/neighbors.html#id5>.
- [10] C. Reinders, H. Ackermann, M. Y. Yang, and B. Rosenhahn, “Chapter 4 - Learning Convolutional Neural Networks for Object Detection with Very Little Training Data,” in *Multimodal Scene Understanding*, M. Y. Yang, B. Rosenhahn, and V. Murino, Eds., Academic Press, 2019, pp. 65–100, ISBN: 978-0-12-817358-9. DOI: <https://doi.org/10.1016/B978-0-12-817358-9.00010-X>. [Online]. Available: <http://www.sciencedirect.com/science/article/pii/B978012817358900010X>.
- [11] L. Tan, “Chapter 17 - Code Comment Analysis for Improving Software Quality,” in *The Art and Science of Analyzing Software Data*, C. Bird, T. Menzies, and T. Zimmermann, Eds., This chapter contains figures, tables, and text copied from the author’s PhD dissertation and the papers that the author of this chapter coauthored [[3], [1], [35], [7]]. Sections 17.2.3, 17.4.3, 17.5, and 17.6 are new, and the other sections are augmented, reorganized, and improved., Boston: Morgan Kaufmann, 2015, pp. 493–517, ISBN: 978-0-12-411519-4. DOI: <https://doi.org/10.1016/B978-0-12-411519-4.00017-3>. [Online]. Available: <http://www.sciencedirect.com/science/article/pii/B9780124115194000173>.
- [12] S. Wallace, *Perl Graphics Programming: Creating Svg, SWF (Flash), JPEG and PNG Files with Perl*. OREILLY MEDIA, Dec. 1, 2002, 478 pp., ISBN: 059600219X. [Online]. Available: [https://www.ebook.de/de/product/3251138/shawn\\_wallace\\_perl\\_graphics\\_programming\\_creating\\_svg\\_swf\\_flash\\_jpeg\\_and\\_png\\_files\\_with\\_perl.html](https://www.ebook.de/de/product/3251138/shawn_wallace_perl_graphics_programming_creating_svg_swf_flash_jpeg_and_png_files_with_perl.html).
- [13] F. Pedregosa, G. Varoquaux, A. Gramfort, V. Michel, B. Thirion, O. Grisel, M. Blondel, P. Prettenhofer, R. Weiss, V. Dubourg, J. Vanderplas, A. Passos, D. Cournapeau, M. Brucher, M. Perrot, and E. Duchesnay, “Scikit-learn: Machine Learning in Python,” *Journal of Machine Learning Research*, vol. 12, no. 85, pp. 2825–2830, 2011. [Online]. Available: <http://jmlr.org/papers/v12/pedregosa11a.html>.
- [14] Michelle, *What exactly is TensorFlow?* English, Access date: 12/15/2020, Medium, Oct. 2018. [Online]. Available: <https://medium.com/datadriveninvestor/what-exactly-is-tensorflow-80a90162d5f1>.
- [15] TensorFlow, *TensorFlow Lite guide*, English, comp. software, Access date: 12/15/2020, TensorFlow, Mar. 2020. [Online]. Available: <https://www.tensorflow.org/lite/guide>.
- [16] Apple, *Swift. the powerful programming language that is also easy to learn*. English, Tech. Rep., Access date: 12/15/2020, Apple. [Online]. Available: <https://developer.apple.com/swift/>.
- [17] C. Bohon, *Apple’s Swift programming language*, English, Access date: 12/15/2020, TechRepublic, Sep. 2020. [Online]. Available: <https://www.techrepublic.com/article/apples-swift-programming-language-the-smart-persons-guide/>.
- [18] Apple Insider, *Xcode*, English, Tech. Rep., Access date: 12/15/2020, Apple insider, Dec. 2020. [Online]. Available: <https://appleinsider.com/inside/xcode>.
- [19] Apple, *Introducing Xcode 12*, English, tech report, Access date: 12/15/2020, Apple. [Online]. Available: <https://developer.apple.com/xcode/>.
- [20] CocoaPods, *What is CocoaPods*, English, comp. software, Access date: 01/15/2021, CocoaPods. [Online]. Available: <https://guides.cocoapods.org/using/getting-started.html>.
- [21] D. J. Lary, G. K. Zewdie, X. Liu, D. Wu, E. Levetin, R. J. Allee, N. Malakar, A. Walker, H. Mussa, A. Mannino, and D. Aurin, “Machine Learning Applications for Earth Observation,” in *Earth Observation Open Science and Innovation*, C. Mathieu Pierre-Philippe and Aubrecht, Ed., Cham: Springer International Publishing, 2018, pp. 165–218, ISBN: 978-3-319-65633-5. DOI: 10.

- 1007/978-3-319-65633-5\_8. [Online]. Available: [https://doi.org/10.1007/978-3-319-65633-5\\_8](https://doi.org/10.1007/978-3-319-65633-5_8).
- [22] X. Ran, L. Xue, Y. Zhang, Z. Liu, X. Sang, and J. He, "Rock Classification from Field Image Patches Analyzed Using a Deep Convolutional Neural Network," *Mathematics*, vol. 7, no. 8, p. 755, 2019. DOI: 10.3390/math7080755.
  - [23] G. Cheng and W. Guo, "Rock images classification by using deep convolution neural network," *Journal of Physics: Conference Series*, vol. 887, p. 012089, 2017. DOI: 10.1088/1742-6596/887/1/012089.
  - [24] G. Fan, F. Chen, D. Chen, and Y. Dong, "Recognizing Multiple Types of Rocks Quickly and Accurately Based on Lightweight CNNs Model," *IEEE Access*, vol. 8, pp. 55269–55278, 2020. DOI: 10.1109/access.2020.2982017.
  - [25] G. Fan, F. Chen, D. Chen, Y. Li, and Y. Dong, "A Deep Learning Model for Quick and Accurate Rock Recognition with Smartphones," *Mobile Information Systems*, vol. 2020, pp. 1–14, 2020. DOI: 10.1155/2020/7462524.
  - [26] Y. Zhang, M. Li, S. Han, Q. Ren, and J. Shi, "Intelligent Identification for Rock-Mineral Microscopic Images Using Ensemble Machine Learning Algorithms," *Sensors*, vol. 19, no. 18, p. 3914, 2019. DOI: 10.3390/s19183914.
  - [27] J. Maitre, K. Bouchard, and L. P. Bédard, "Mineral grains recognition using computer vision and machine learning," *Computers & Geosciences*, vol. 130, pp. 84–93, 2019. DOI: 10.1016/j.cageo.2019.05.009.
  - [28] P. Dangeti, *Statistics for Machine Learning*. Packt Publishing, Jul. 21, 2017, 442 pp., ISBN: 1788295757. [Online]. Available: [https://www.ebook.de/de/product/29829428/pratap\\_dangeti\\_statistics\\_for\\_machine\\_learning.html](https://www.ebook.de/de/product/29829428/pratap_dangeti_statistics_for_machine_learning.html).
  - [29] Scikit learn, *Support Vector Classification*, English, Access date: 01/15/2021, Scikit-learn. [Online]. Available: <https://scikit-learn.org/stable/modules/generated/sklearn.svm.SVC.html?highlight=svc#sklearn.svm.SVC>.
  - [30] G. Bonaccorso, A. Fandango, and R. Shanmugamani, *Python*. Packt Publishing, Dec. 19, 2018, 764 pp., ISBN: 1789957214. [Online]. Available: [https://www.ebook.de/de/product/35139551/giuseppe\\_bonaccorso\\_armando\\_fandango\\_rajalingappaa\\_shanmugamani\\_python.html](https://www.ebook.de/de/product/35139551/giuseppe_bonaccorso_armando_fandango_rajalingappaa_shanmugamani_python.html).
  - [31] A. Mishra, *Metrics to evaluate your machine learning algorithm*, English, Access date: 12/22/2020, Medium, Feb. 2018. [Online]. Available: <https://towardsdatascience.com/metrics-to-evaluate-your-machine-learning-algorithm-f10ba6e38234>.

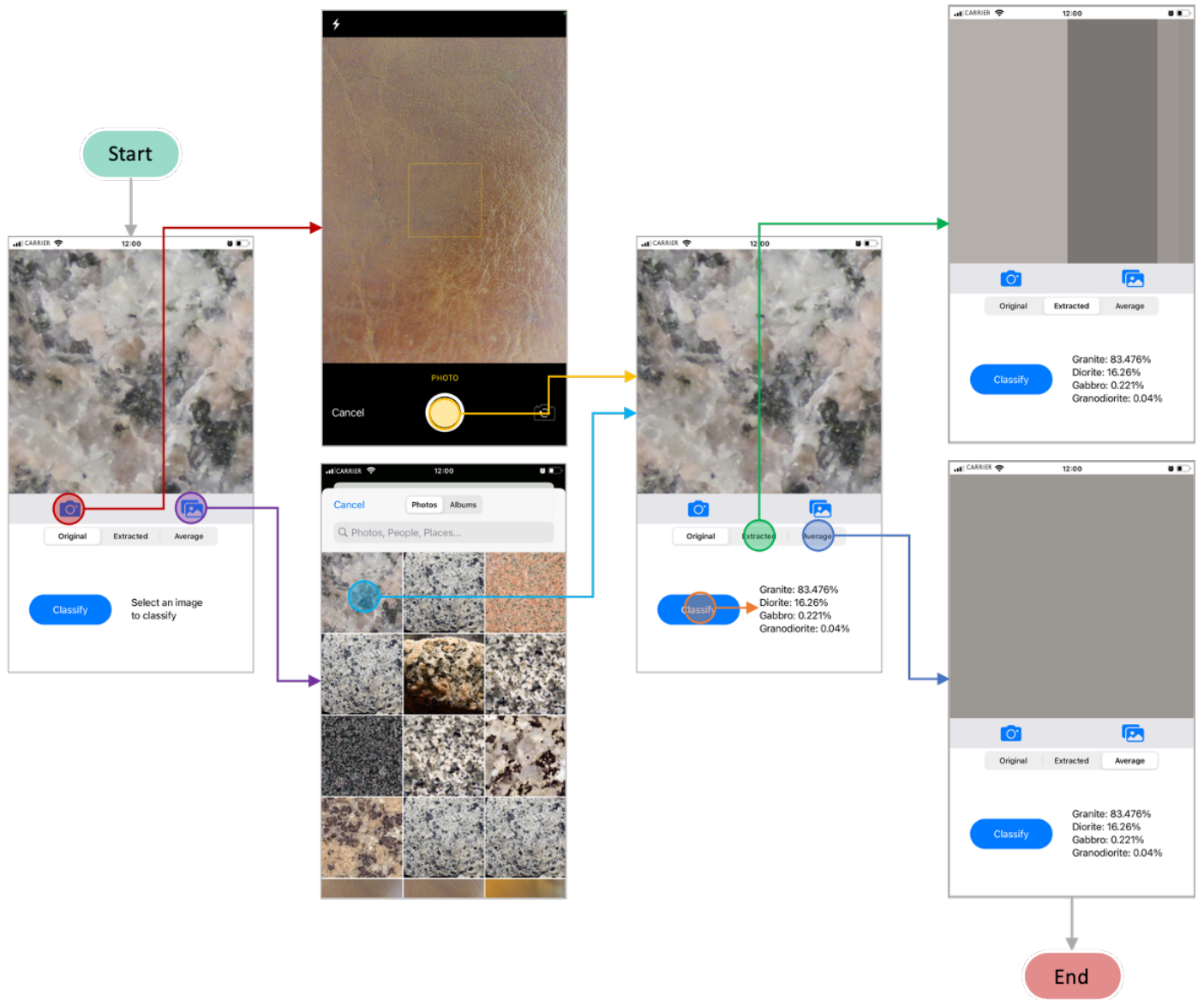


Figure 4. Application workflow